

KK258, a new transition dwarf galaxy neighbouring the Local Group ^{*} †

I. D. Karachentsev^{1‡}, L. N. Makarova¹, R. B. Tully², Po-Feng Wu², A. Y. Kniazev^{3,4,5}

¹Special Astrophysical Observatory, Nizhniy Arkhiz, Karachai-Cherkessia 369167, Russia

²Institute for Astronomy, University of Hawaii, 2680 Woodlawn Drive, HI 96822, USA

³South African Astronomical Observatory, PO Box 9, 7935 Observatory, Cape Town, South Africa.

⁴Southern African Large Telescope Foundation, PO Box 9, 7935 Observatory, Cape Town, South Africa.

⁵Sternberg Astronomical Institute, Lomonosov Moscow State University, Moscow, Russia

Accepted XXX. Received XXX; in original form XXX

ABSTRACT

Here we present observations with the Advanced Camera for Surveys on the Hubble Space Telescope of the nearby, transition-type dwarf galaxy KK258 = ESO468-020. We measure a distance of 2.23 ± 0.05 Mpc using the Tip of Red Giant Branch method. We also detect H α emission from this gas-poor dwarf transition galaxy at the velocity $V_h = 92 \pm 5$ km s⁻¹ or $V_{LG} = 150$ km s⁻¹. With this distance and velocity, KK258 lies near the local Hubble flow locus with a peculiar velocity ~ 3 km s⁻¹. We discuss the star formation history of KK258 derived from its colour-magnitude diagram. The specific star formation rate is estimated to be $\log[\text{sSFR}] = -2.64$ and -2.84 (Gyr⁻¹) from the FUV-flux and H α -flux, respectively. KK258 has the absolute magnitude $M_B = -10.3$ mag, the average surface brightness of 26.0 mag arcsec⁻² and the hydrogen mass $\log(M_{HI}) < 5.75 M_\odot$. We compare KK258 with 29 other dTr- galaxies situated within 5 Mpc from us, and conclude that its properties are typical for transition dwarfs. However, KK258 resides 0.8 Mpc away from its significant neighbour, the Sdm galaxy NGC 55, and such a spatial isolation is unusual for the local transition dwarfs.

Key words: galaxies: dwarf – galaxies: distances and redshifts – galaxies: stellar content – galaxies: individual: KK258

1 INTRODUCTION

Special sky surveys for dwarf galaxies in the wide vicinities of M 31 (Ibata et al. 2007; Martin et al. 2009; Ibata et al. 2014) and M 81 (Chiboucas et al. 2009, 2013) led over a short time to a doubling of the number of dwarf companions to these nearest giant spiral galaxies. Significant additions to the family of dwarf satellites of the Milky Way has been arising over the last years due mainly to the wide-field sky surveys: Sloan Digital Sky Survey (SDSS, Abazajian et al. (2009)) and Panoramic Survey Telescope and Rapid Response System 1 (Pan-STARRS1, Tonry et al. (2012)) - see a comprehensive overview by McConnachie (2012).

The sport of hunting for nearby dwarfs is invigorated

by the challenge to resolve the known contradiction between the few observed companions around local massive galaxies and the great amount of them from theoretical expectations (Klypin et al. 1999), that exceed by tenfold the observed numbers. Still, there are observational constraints beyond 1 Mpc because the limiting apparent magnitude of the SDSS and Pan-STARRS surveys turns out to be insufficient to resolve into stars the old population of dwarfs residing outside the Local Group (LG).

Analysing data on radial velocities and distances of 30 galaxies located between 1 and 3 Mpc, Karachentsev et al. (2009) showed that the Hubble flow around the LG is rather "cold" with a peculiar velocity dispersion of $\sigma_V \simeq 25$ km s⁻¹. Over the last 5 years, in the spherical layer within $D = 1 - 3$ Mpc only 2 new dwarf galaxies were found: UGC4879 (Kopylov et al. 2008; Jacobs et al. 2011; Kirby et al. 2012) and Leo P (Rhode et al. 2013; McQuinn et al. 2013; Giovanelli et al. 2013). Here, we report on the discovery of a third dwarf system, KK 258, situated at 0.80 Mpc separation from NGC 55, in a low-density region between the LG and NGC 253 group in Sculptor.

The interest in such solitary objects is due to an ap-

^{*} Based on observations made with the NASA/ESA Hubble Space Telescope, program GO-12546, with data archive at the Space Telescope Science Institute. STScI is operated by the Association of Universities for Research in Astronomy, Inc. under NASA contract NAS 5-26555.

[†] Based on observations made with the Southern African Large Telescope (SALT).

[‡] E-mail: ikar@sao.ru

preciation that they have not forgotten their "initial conditions" unlike virialized members of groups. Discovering even one isolated dwarf with a high peculiar velocity could disprove the coldness of the local Hubble flow with important cosmological implications.

The low surface brightness dwarf galaxy KK 258 = ESO468-020 was included in the Neighboring Galaxy Catalog (Karachentsev et al. 2004) as having a distance of 3.9 Mpc based on its supposed association with the giant spiral galaxy NGC 253. However an accurate measurement of the distance from the luminosities of stars at the tip of the red giant branch reveals that KK 258 is well to the foreground, at only half its expected distance.

2 ACS HST OBSERVATIONS AND TRGB DISTANCE

Observations of KK258 were carried out with the Advanced Camera for Surveys on the Hubble Space Telescope on August 12, 2012 as a part of SNAP project 12546 (PI: R.B.Tully). Two images were obtained in the F606W and F814W filters with exposures 900 s in each. The F606W image of the galaxy is shown in Figure 1. We use the ACS module of the DOLPHOT software package by A.Dolphin (<http://purcell.as.arizona.edu/dolphot>) to do photometry of resolved stars as well as run artificial star tests to characterize the completeness and uncertainty in the measurements. The data quality images were used to mask bad pixels. Only stars with photometry of good quality were used in the analysis. The resulting colour-magnitude diagram (CMD) in F606W – F814W versus F814W is plotted in Figure 2.

Then, we use a maximum-likelihood method from Makarov et al. (2006) to measure the magnitude of the tip of the red giant branch (TRGB) in KK258 and find $F814W(TRGB) = 22.79 \pm 0.04$. Following the zero-point calibration of the absolute magnitude of the TRGB developed by Rizzi et al. (2007), we obtain $M(TRGB) = -4.09$. Using these values and accounting for foreground reddening of $E(B-V) = 0.011$ from Schlafly & Finkbeiner (2011), we derive a distance of $(m - M)_0 = 26.85 \pm 0.07$ or $D = 2.23 \pm 0.05$ Mpc.

3 METALLICITY AND STAR FORMATION HISTORY

We determine the quantitative star formation and metal enrichment history of KK258 from its CMD (STARPROBE program). Our program determines an approximation of the observed distribution of stars in the CMD, using a positive linear combination of synthetic diagrams formed by simple stellar populations (SSP). A full description of the details of our approach and the algorithm are given in the papers of Makarov & Makarova (2004); Makarova et al. (2010).

The observed data were binned into Hess diagrams, giving the number of stars in cells of the CMDs. Also synthetic Hess diagrams were constructed from theoretical stellar isochrones and initial mass function (IMF). We used the Padova2000 set of theoretical isochrones (Girardi et al. 2000), and a Salpeter (1955) IMF. The synthetic diagrams

were altered by the same incompleteness and crowding effects, and photometric systematics as those determined for the observations using artificial star experiments. We used the distance modulus determined in the present paper. We have taken into account the presence of unresolved binary stars (binary fraction). Following Barmina et al. (2002), the binary fraction was taken to be 30 per cents. The mass function of individual stars and the main component of a binary system is supposed to be the same. The mass distribution for the second component was taken to be flat in the range 0.7 to 1.0 of the main component mass. The best fitting combination of synthetic CMDs is a maximum-likelihood solution taking into account the Poisson noise of star counts in the cells of the Hess diagram. The result of our calculations of the star formation history of KK258 is shown in Figure 3.

The main starburst in KK258 apparently occurred 12 – 14 billion years ago. The average rate of star formation in this period was $7.9_{-3.2}^{+4.8} \times 10^{-3} M_{\odot}/yr$. The average metallicity of the stars formed is quite low, $[Fe/H] \simeq -1.6$. The bulk of the stellar mass of the galaxy was formed during this initial starburst. We estimate the mass fraction formed during this initial event to be 70 per cent. The total stellar mass formed during the galaxy life amounts to $2.2 \times 10^7 M_{\odot}$. Faint traces of star formation are indicated in the time intervals of [6 – 8] and [2 – 4] Gyr ago. A marked enhancement of star formation likely occurred in a short period 1.5 – 2 billion years ago. The metallicity of these stars is slightly higher: $[Fe/H] \simeq -1.0$.

A very weak but reliable sign of star formation is seen in the last billion years. The average star formation rate in this recent period is $3.8_{-1.0}^{+3.0} \times 10^{-4} M_{\odot}/yr$. A very small number of stars continue to be formed at the current time.

4 H α EMISSION AND RADIAL VELOCITY

In the course of a survey of nearby galaxies in the H α line with the 6-meter telescope of the Special Astrophysical Observatory, Russian Academy of Sciences, Kaisin & Karachentsev (2013) imaged KK258 in the H α line and in the neighbouring continuum. This southern object culminated at the zenith distance of 74 degrees (!). After the standard data processing, a faint emissive patch of 5 arcsec size was detected in the central region of KK 258. The integral flux from the patch amounts to $F(H\alpha) = (4.3 \pm 0.9) 10^{-15}$ erg cm $^{-2}$ s $^{-1}$, that at the distance of 2.23 Mpc corresponds to the star formation rate $\log[SFR] = \log F(H\alpha) + 2 \log D + 8.98 = -4.68$ in units of $[M_{\odot}/yr]$ (Kennicutt 1998). This emission knot in the centre of KK 258 is also seen in ultraviolet images obtained with the space GALEX telescope (Gil de Paz et al. 2007). The apparent FUV-magnitude of this knot, $m_{FUV} = 20.0$ mag, after a small correction for the Galactic extinction, yields the star formation rate of $\log[SFR] = -4.48 M_{\odot}/yr$ in good agreement with the estimate from H α emission.

Spectroscopic observations of the H α knot in the KK258 were conducted with the SALT telescope (Buckley et al. 2006; O'Donoghue et al. 2006) on October 23, 2013 with the Robert Stobie Spectrograph (RSS; Burgh et al. 2003; Kobulnicky et al. 2003). To detect the narrow faint H α line the high resolution long-slit spectroscopy mode of the RSS was used with a 2.0 arcsec slit width. The grating GR2300 was

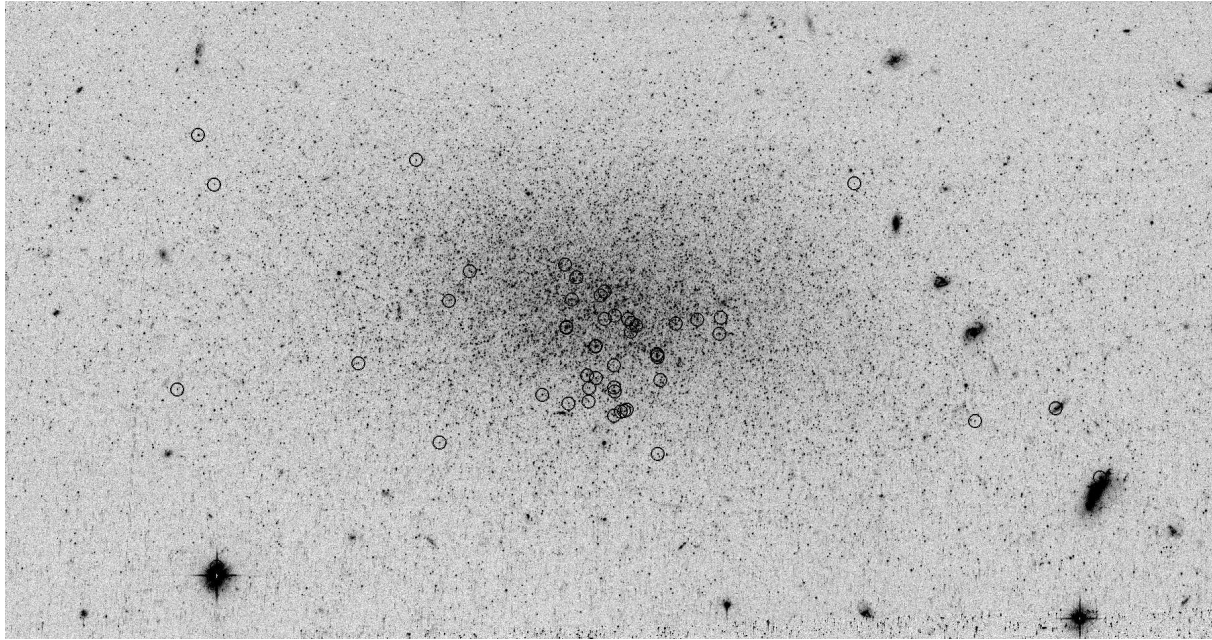


Figure 1. *HST/ACS* image of KK258 in *F606W* filter. The image size is 3.0×1.6 arcmin. Blue stars with $F606W - F814W \leq 0.2$ and $F814W \leq 25.5$ are shown with open circles.

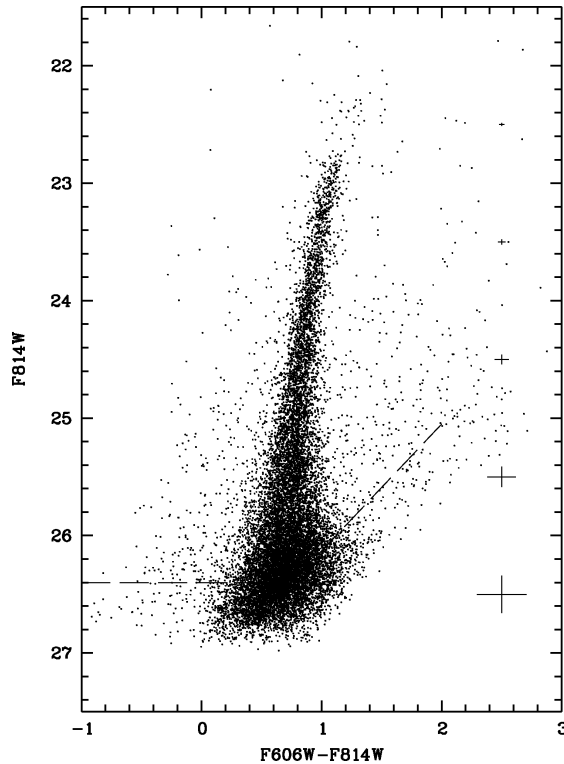


Figure 2. Colour-magnitude diagram of KK258. The photometric errors are indicated with the bars in the right part of the CMD. The stars under the dashed line were not used in the SFH measurements.

used to cover the spectral range $6100\text{--}6900 \text{ \AA}$ with a reciprocal dispersion of $\sim 0.27 \text{ \AA pixel}^{-1}$ and FWHM spectral resolution of $1.39 \pm 0.05 \text{ \AA}$. The seeing during the observation was ≈ 2.5 arcsec. The RSS pixel scale is 0.127 arcsec and the effective field of view is 8 arcmin in diameter. We

utilized a binning factor of 4 in the spatial direction, in order to give a final sampling of $0.51 \text{ arcsec pixel}^{-1}$. The total exposure time was 1950 s, which was broken up into 3 sub-exposures, 650 s each, to allow for removal of cosmic rays. A spectrum of Ne comparison arcs was obtained to calibrate

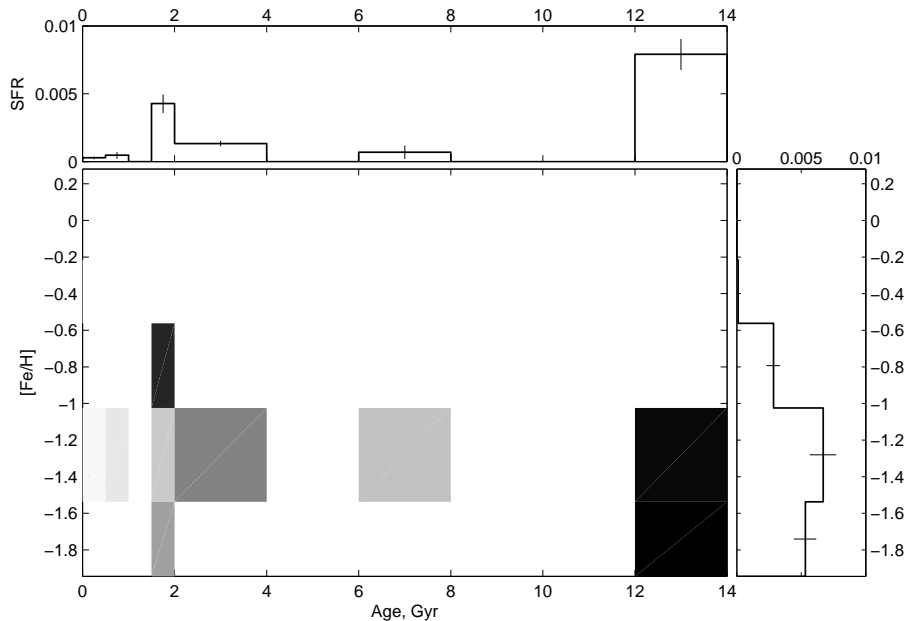


Figure 3. The star formation history of KK258. Top panel shows the star formation rate (SFR) (M_{\odot}/yr) against the age of the stellar populations. The bottom panel represents the metallicity of stellar content as a function of age. The right panel is SFR vs. metallicity. The resulting errors in SFR are indicated with the vertical bars.

the wavelength scale. Primary reduction of the data was done with the SALT science pipeline (Crawford et al. 2010). The long-slit reduction was done later, in the way described in Kniazev et al. (2008). We would like to note that SALT is a telescope with a variable pupil, and its illuminated beam changes continuously during the observations. This makes the absolute flux/magnitude calibration impossible, even using spectrophotometric standard stars.

As seen from the data, there is a faint emission line with equivalent width of $EW \simeq 3.3\text{\AA}$ at the wavelength 6565\AA . The one-dimensional scan of the spectrum in the range of $6550\text{--}6580\text{\AA}$ is presented in Figure 4. Identification of this emission detail with the $H\alpha$ line yields the heliocentric velocity $V_h = 92 \pm 5\text{ km s}^{-1}$ or the Local Group centroid velocity $V_{LG} = 150\text{ km s}^{-1}$.

5 KK258 AND THE LOCAL HUBBLE FLOW

The data on galaxies that outline the Hubble flow around the LG are presented in Table 1. The nearby galaxies are selected using two conditions: a) distance of the galaxy from the LG centroid is within 3.5 Mpc, b) tidal index of the galaxy θ_1 is less than +0.2, that avoid selecting objects in groups with appreciable virial velocities. The data are taken from UNGC catalogue (Karachentsev et al. 2013) which contains references to the data sources given in Tables 4 - 7. For several objects: SexB, SexA, NGC3741 and DDO210 their UNGC-distances were replaced by values from the Extragalactic Distance Database (Tully et al. 2009; Jacobs et al. 2009). The Table columns contain: (1) galaxy name, (2),(3) equatorial coordinates at the epoch (J2000.0), (4) distance from the MW and its error, (5) distance from the LG barycenter assuming its location on the line between the MW and M31 at a distance of 0.43 Mpc away from the MW

(Karachentsev et al. 2009), (6) heliocentric radial velocity in km s^{-1} , (7) velocity in the LG rest frame with the apex parameters adopted in the NASA Extragalactic Database (NED, <http://ned.ipac.caltech.edu>), (8) the tidal index

$\Theta_1 = \max[\log(M_n^*/D_n^3)] - 10.96$, $n=1,2,\dots,N$, where M_n^* is a stellar mass of n -rank neighbour, and D_n is its separation from the considered galaxy (Karachentsev et al. 2013). Apart from 35 galaxies listed in Table 1, there are three more galaxies with low velocities V_{LG} : 199 km s^{-1} (UGC6757), 196 km s^{-1} (LVJ1213+2957), and 145 km s^{-1} (UGC8245), however, their distances remain unmeasured.

The relation between the radial velocities and distances of the 35 nearest isolated galaxies is shown in Figure 5 by solid circles with horizontal bars indicating the distance errors. The dwarf system KK 258 as a new member of the local Hubble flow is distinguished by a star. The dashed line corresponds to the unperturbed Hubble flow with a parameter $H_0 = 73\text{ km s}^{-1}\text{ Mpc}^{-1}$. The solid line represents the regression of radial velocity on distance for a canonic Lemetre-Tolman model with the parameter $R_0 = 0.9\text{ Mpc}$, that indicates the radius of the sphere of zero velocity around the LG. As seen, KK 258 lies close to the regression line. It has a peculiar velocity only $V_{pec} \sim 3\text{ km s}^{-1}$, comparable with the distance measurement error of $\sigma_D H_0 \simeq 8\text{ km s}^{-1}$ and the radial velocity error of 5 km s^{-1} .

Note that several galaxies on the local Hubble diagram: DDO 99, DDO 125, DDO 181, UGC 8833, and DDO 190, members of the dwarf associations 14+7 and 14+8 (Tully et al. 2006), reside in the Canes Venatici constellation and exhibit an effect of bulk motion toward the nearby CVn-I cloud with a velocity of 55 km s^{-1} . For the remaining galaxies the peculiar velocity scatter is only 28 km s^{-1} , and about 10 km s^{-1} of this quantity is caused by the distance errors.

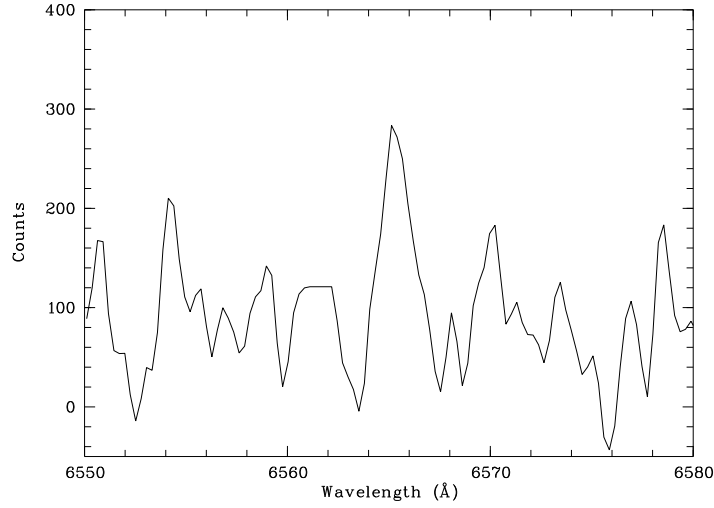


Figure 4. One-dimensional scan of the spectrum of KK258.

Table 1. The Local Hubble flow galaxies

Galaxy	RA	DEC	D_{MW}	Err	D_{LG}	V_h	V_{LG}	Θ_1
(1)	(2)	(3)	(4)	(5)	(6)	(7)	(8)	(9)
	J2000.0		Mpc		Mpc	km s ⁻¹	km s ⁻¹	
WLM= DDO221	00 01 58.1	-15 27 40	0.97	0.02	0.82	-122	-16	0.0
ESO349-031	00 08 13.3	-34 34 42	3.21	0.16	3.10	221	230	0.0
NGC0055	00 15 08.5	-39 13 13	2.13	0.10	2.10	129	111	0.1
NGC0300	00 54 53.5	-37 40 57	2.15	0.10	2.11	146	116	0.1
NGC0404	01 09 26.9	+35 43 03	3.05	0.15	2.63	-50	193	-0.8
HIZSS003	07 00 29.3	-04 12 30	1.67	0.17	1.79	288	108	-1.1
NGC2403	07 36 51.4	+65 35 58	3.18	0.16	3.15	125	262	0.2
UGC04879	09 16 02.2	+52 50 24	1.36	0.06	1.34	-25	33	-0.7
LeoA= DDO69	09 59 26.4	+30 44 47	0.80	0.04	0.96	24	-40	-0.1
SexB= DDO70	10 00 00.1	+05 19 56	1.43	0.07	1.69	300	110	-0.8
NGC3109	10 03 07.2	-26 09 36	1.32	0.06	1.68	403	110	0.2
SexA= DDO75	10 11 00.8	-04 41 34	1.43	0.07	1.74	324	94	-0.8
LeoP	10 21 45.1	+18 05 17	2.00	0.30	2.24	262	135	-1.3
NGC3741	11 36 06.4	+45 17 07	3.22	0.16	3.34	229	263	-0.7
DDO99	11 50 53.0	+38 52 50	2.64	0.14	2.74	251	257	-0.8
IC3104	12 18 46.1	-79 43 34	2.27	0.19	2.61	429	170	-1.2
DDO125	12 27 41.8	+43 29 38	2.74	0.14	2.81	206	251	-0.8
GR8= DDO155	12 58 40.4	+14 13 03	2.13	0.11	2.39	217	139	-1.4
UGC08508	13 30 44.4	+54 54 36	2.69	0.14	2.67	56	181	-0.8
DDO181= U8651	13 39 53.8	+40 44 21	3.01	0.15	3.08	214	284	-1.1
DDO183= U8760	13 50 51.1	+38 01 16	3.22	0.16	3.38	188	254	-1.0
KKH86	13 54 33.6	+04 14 35	2.59	0.13	2.89	287	209	-1.4
UGC08833	13 54 48.7	+35 50 15	3.08	0.15	3.24	221	280	-1.1
KK230= KKR03	14 07 10.7	+35 03 37	2.14	0.10	2.26	63	127	-1.3
DDO187= U9128	14 15 56.5	+23 03 19	2.24	0.12	2.43	160	180	-1.4
DDO190= U9240	14 24 43.5	+44 31 33	2.80	0.14	2.84	150	263	-1.2
KKR25	16 13 47.6	+54 22 16	1.86	0.12	1.79	-79	128	-1.0
IC4662	17 47 06.3	-64 38 25	2.44	0.18	2.74	302	139	-1.3
SagdIr=ESO594-4	19 29 59.0	-17 40 41	1.04	0.07	1.14	-79	21	-0.4
DDO210=Aquarius	20 46 51.8	-12 50 53	0.98	0.05	0.97	-140	11	-0.3
IC5152	22 02 41.9	-51 17 43	1.97	0.12	2.08	122	73	-1.3
KK258=ESO468-20	22 40 43.9	-30 47 59	2.23	0.11	2.34	92	150	-1.1
Tucana	22 41 49.0	-64 25 12	0.88	0.04	1.09	194	73	-0.2
UGCA438	23 26 27.5	-32 23 26	2.18	0.12	2.11	62	99	-0.4
KKH98	23 45 34.0	+38 43 04	2.52	0.13	2.11	-132	156	-0.9

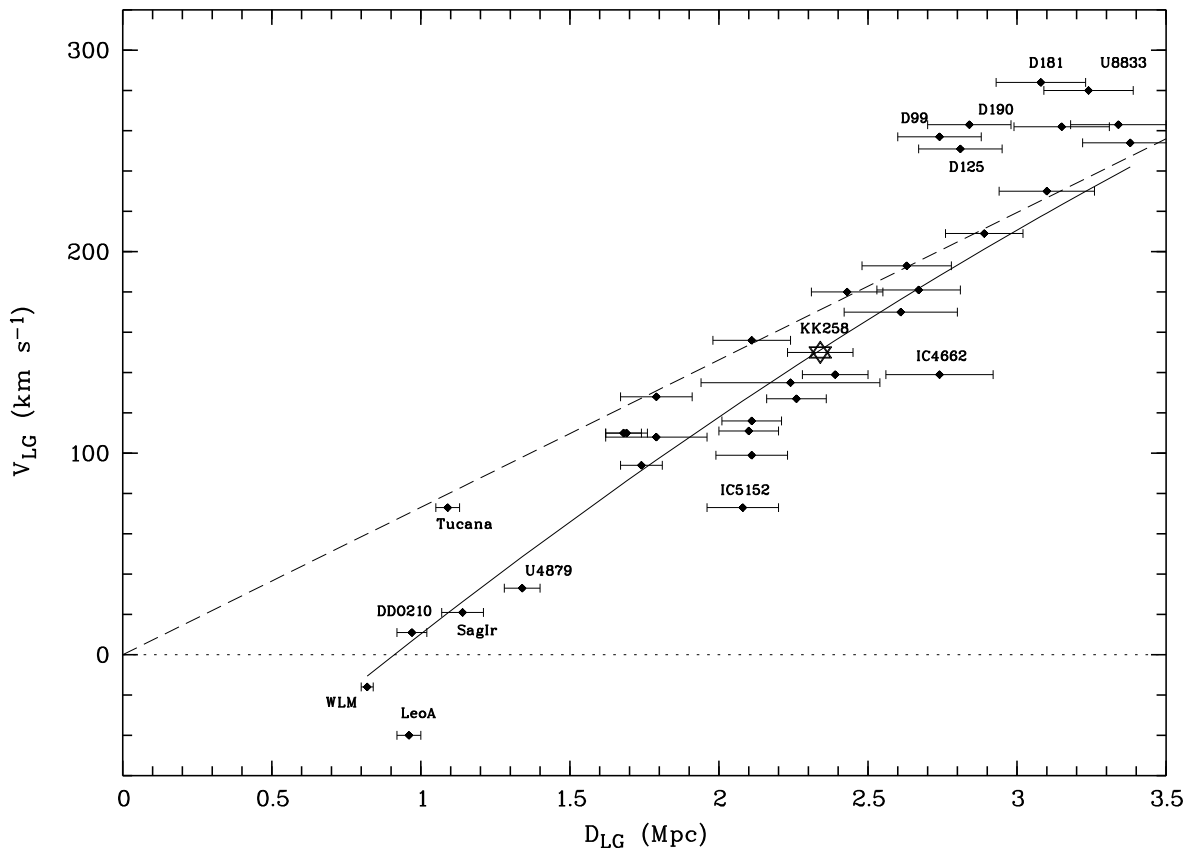


Figure 5. Relation between radial velocities and distances of the 35 nearest isolated galaxies.

6 KK258 VS. OTHER NEARBY TRANSITION DWARFS

According to a common point of view, a "transition" type dwarf is a galaxy dominated by the old population but manifesting signs of recent star formation. This definition implies the knowledge of detailed star formation history derived from a reasonably deep CMD. However, the deep CMDs are available mostly for the nearest dwarfs. Given the set of attributes – low hydrogen content, low rate of recent star formation and low surface brightness – the dwarf system KK 258 belongs to the transition type, intermediate between irregular (dIr) dwarfs and spheroidals (dSph). There is a widespread view that the dwarf transition (=dTr) systems are forming from dIrs via their gas depletion, whereupon star formation fades. It is usually considered that a dying dwarf of the dTr- type transforms with time into a spheroidal dwarf if it is not fed by gas from the intergalactic medium. Individual properties of some nearby dTr dwarfs have been discussed by Hidalgo et al. (2013) and Yang et al. (2014). For obvious reasons, classification of intermediate morphology dwarfs faces substantial difficulties. One can cite many cases where dTr dwarfs were attributed to the dIr or dSph type. An example of questionable classification is the case of nearby dIr galaxy UGC 4879 attributed to dTr type by (Kirby et al. 2012). Another examples of difficulty classifying dTr are the nearby dwarf galaxies Cetus and Tucana. Based on the luminosity- metallicity relation for the Local Group

dwarfs, Yang et al. (2014) attributed Cetus and Tucana to the transition type, while Monelli et al. (2010); Weisz et al. (2011); Hidalgo et al. (2013) described them as typical dSphs because of their negligible current star formation rate. On the other hand, Karachentsev et al. (2011) found a case when a dwarf galaxy DDO44, usually classified as dSph, contains a small emission knot with a dozen blue stars producing a star formation rate of $\text{dex}(-5.1) M_{\odot}/\text{yr}$.

The UNGC catalogue contains 30 galaxies classified as dTr within a distance of 5 Mpc. Classification of such objects at greater distances becomes uncertain. A summary of the nearest dTr dwarfs is presented in Table 2. The columns represent the following data from UNGC: (1) galaxy name, (2) equatorial coordinates (J2000.0), (3) distance in Mpc, (4) method used to derive the distance: TRGB - via the tip of the red giant branch, SBF - via surface brightness fluctuations, mem - via the group membership, txt - via texture of galaxy image, (5) absolute B-magnitude corrected for the Galactic extinction according to Schlegel et al. (1998), (6) average surface brightness within the Holmberg isophote, (7) logarithm of stellar mass derived from the K-band luminosity, (8) logarithm of hydrogen-to-stellar mass ratio, (9) star formation rate in M_{\odot}/yr , (10) specific star formation rate in M_{\odot}/yr normalized by the stellar mass, (11) the tidal index determined by the nearest significant neighbour, (12) the group to which the dwarf galaxy belongs. The last line in Table 2 presents median parameters for the dTr sam-

Table 2. List of 30 transition type dwarf galaxies within 5.0 Mpc

Name	J2000.0	D	meth	M_B	SB	$\lg(M_*)$	$\lg(M_{HI}/M_*)$	$\lg(\text{SFR})$	$\lg(\text{sSFR})$	Θ_1	Group
(1)	(2)	(3)	(4)	(5)	(6)	(7)	(8)	(9)	(10)	(11)	(12)
ESO410-005	001531.4–321048	1.92	TRGB	−11.6	24.5	6.88	−0.97	−3.97	−10.85	0.0	N55
Cetus	002611.0–110240	0.78	TRGB	−10.2	26.3	7.02	< −2.84	< −6.54	< −13.56	0.3	M31
ESO294-010	002633.3–415120	1.92	TRGB	−10.9	25.0	6.25	−0.77	−3.86	−10.11	0.4	N55
KDG002	004921.1–180428	3.40	TRGB	−11.4	25.4	6.81	−0.86	−3.87	−10.68	0.5	N253
LGS 3	010355.0+215306	0.65	TRGB	−9.3	25.4	5.96	−0.94	−5.23	−11.19	1.5	M31
Phoenix	015106.3–442641	0.44	TRGB	−9.6	26.0	6.08	< −0.86	−4.43	−10.51	0.7	MW
UGC01703	021255.8+324851	4.19	SBF	−11.5	24.9	7.56	< −1.26	< −4.85	< −12.41	−1.3	–
[KK2000] 03	022442.7–733046	4.10	mem	−12.3	26.4	8.21	< −1.93	< −5.02	< −13.23	−0.8	–
KKH22	034456.6+720352	3.50	mem	−11.4	25.8	6.80	< −0.34	< −4.05	< −10.85	1.1	IC342
CKT09d0926+70	092627.9+703024	3.40	TRGB	−9.6	25.1	6.11	< −0.59	−4.30	−10.41	1.7	M81
CKT09d0939+71	093915.9+711842	3.75	TRGB	−8.4	25.8	5.63	–	−5.76	−11.39	2.0	M81
CKT09d0944+71	094434.4+712857	3.36	TRGB	−11.1	25.0	7.38	< −1.90	−5.74	−13.12	1.6	M81
Antlia	100404.0–271955	1.32	TRGB	−9.8	26.1	6.49	−0.55	−3.56	−10.05	2.3	N3109
KDG063	100507.3+663318	3.50	TRGB	−12.1	25.9	7.80	−0.89	< −5.02	< −12.82	2.0	M81
KDG064	100701.9+674939	3.70	TRGB	−12.6	25.4	7.98	–	−5.52	−13.50	2.7	M81
CKT09d1014+68	101455.8+684527	3.84	TRGB	−7.9	25.2	6.12	< −0.43	−4.73	−10.85	2.0	M81
CKT09d1015+69	101506.9+690215	3.87	TRGB	−7.6	26.0	6.01	–	−5.43	−11.44	1.3	M81
HS117	102125.2+710658	3.96	TRGB	−11.2	26.5	6.72	−1.71	−4.32	−11.04	1.2	M81
KDG090	121457.9+361308	2.86	TRGB	−11.5	25.4	6.86	< −1.30	< −5.44	< −12.30	1.3	N4214
[KK2000] 51	124421.5–425623	3.60	mem	−10.9	24.4	6.60	< −0.28	< −5.01	< −11.61	0.8	N5128
KK166	124913.3+353645	4.74	TRGB	−10.8	25.1	7.28	–	< −5.02	< −12.30	0.7	N4736
KDG218	130544.0–074520	5.00	txt	−11.9	26.6	7.71	< −1.10	−4.85	−12.56	−1.0	–
NGC5011C	131311.9–431556	3.60	mem	−14.1	22.9	7.95	< −0.83	−3.39	−11.34	2.0	N5128
[KK2000] 54	132132.4–315311	4.60	mem	−10.5	25.7	6.44	< −0.66	< −4.87	< −11.31	0.9	N5236
KK198	132256.1–333422	4.60	mem	−11.0	24.7	7.34	< −1.52	−4.26	−11.60	0.8	N5236
AM1320-230	132329.9–232335	4.60	mem	−11.1	25.2	7.41	< −1.63	−4.32	−11.73	0.4	N5236
KK203	132728.1–452109	3.60	mem	−10.5	24.6	6.46	< −0.14	< −4.97	< −11.43	2.0	N5128
And XXVIII	223241.2+311258	0.65	TRGB	−7.7	26.3	6.04	–	< −6.60	< −12.64	1.1	M31
KK258	224043.9–304759	2.23	TRGB	−10.3	26.0	7.16	< −1.41	−4.48	−11.64	−1.1	–
Tucana	224149.0–642512	0.88	TRGB	−9.2	26.5	6.62	< −2.44	−6.04	−12.66	−0.2	MW
Median	–	3.5	–	−10.9	25.4	6.80	< −1.0	< −4.8	< −11.7	0.9	–

ple. The typical transition dwarf has the absolute magnitude $M_B = -10.8$ and a stellar mass $\log M_* = 6.8$. Apparently, galaxies with such a shallow potential well easily loose their gaseous component during the first immersion into the dense regions of the massive neighbour. Judging from the median quantity $\theta_1=0.9$, the majority of transition dwarfs are in the close neighbourhood of their main disturbers. The typical hydrogen-to-stellar mass ratio for these galaxies does not exceed 10 per cent, and the observed low star formation rate can only reproduce $\sim 1/30$ part of the stellar mass of dTrs over the cosmic time $T_0=13.7$ Gyr. Among the 30 objects of the sample, two dwarf systems: Phoenix and Tucana are peripheral satellites of the MW, three dTrs: Cetus, LGS-3 and And XXVIII belong to the M 31 suite, and eight transition dwarfs are members of the M 81 group.

Figure 6 presents a mosaic of histograms which reproduce distributions of 30 dTr galaxies according to different parameters. The galaxy KK 258 is marked in black. The upper limits for $M(\text{HI})$ and SFR are shaded. KK 258 looks like a typical representative of the sample according to the majority of parameters: luminosity, surface brightness, relative hydrogen abundance and star formation rate. The only difference of KK 258 from other dTr dwarfs appears in its tidal index, $\Theta_1 = -1.1$. In the UNGC, the nominally nearest significant neighbour to KK 258, i.e. its Main Disturber,

is NGC 253 but, as discussed in the next section, good distances reveal that these galaxies are not associated.

7 KK 258 ENVIRONMENT

Figure 7 demonstrates the distribution of known galaxies within a distance of 3 Mpc around the NGC 55 group in Supergalactic coordinates. The galaxies are shown by solid circles with their names labelled. Three giant galaxies: the Milky Way, M 31 and NGC 253 having absolute magnitudes $M_B < -20.0$ mag are distinguished by large open circles. The dwarf object KK 258 is marked by a star. The upper panel presents the local landscape in the Supergalactic plane, SGX, SGY. Here objects with $|\text{SGZ}| > 1.0$ Mpc were excluded. The bottom panel shows the galaxy distribution in SGZ, SGY, where objects outside the Sculptor filament with $|\text{SGX}| > 1.5$ Mpc are excluded. The true, physical companions having the positive Θ_1 are bound with their Main Disturber by solid lines, and some probable satellites with $\Theta_1 < 0$ are linked by dashed lines. Two dense clouds of companions around the MW and M31 are delineated by ellipses.

The spatially nearest galaxy to KK 258 is a dwarf irregular galaxy UGCA 438 separated by 0.46 Mpc. This dwarf is a member of the NGC 55 group consisting of 5 members: NGC 55, NGC 300, ESO 294-010, ESO 410-005, and

UGCA 438. Their radial velocities lie in the interval [53 – 116] km s^{-1} . Two other neighbouring dwarf galaxies: IC 5152 and KK 258 with their radial velocities: 73 km s^{-1} and 150 km s^{-1} are distant associates of the NGC 55 group. The Sdm galaxy NGC 55 has a stellar mass of $3.0 \cdot 10^9 M_{\odot}$. According to Makarov & Karachentsev (2011), the NGC 55 group is characterized by a velocity dispersion of only 26 km s^{-1} and the projected (virial) mass of $3.3 \cdot 10^{11} M_{\odot}$ (scaled to the distance of 2.13 Mpc). Including in this group two its outliers KK 258 and IC 5152 increases the velocity dispersion to 31 km s^{-1} and increases the mean projected radius from 245 kpc to 347 kpc, yielding a virial mass of $6.6 \cdot 10^{11} M_{\odot}$. Therefore, the virial mass-to-sum of stellar mass of the NGC 55 group amounts to $6.6 \cdot 10^{11} / 6.4 \cdot 10^9 = 103$. As has been noted already by Tully et al. (2006), the association of dwarfs around the dwarf spiral NGC 55 has a substantial amount of dark matter for the amount of light.

The properties of KK 258 as a representative of the dTr class are unlikely to have been caused by an interaction with a neighbour. The status of the dwarf system KK 258 in the category of dTrs is difficult to ascribe to external, tidal effects. To explain the observed properties of the isolated transition type galaxy KK 258 plausibly one could invoke a scenario of "cosmic web stripping" such as proposed by Benítez-Llambay et al. (2013). Perhaps though, in some fraction of cases, violent events in the early star forming phase drives most gas out of the shallow potential of small galaxies and is never significantly replenished.

8 CONCLUDING REMARKS

In this paper we present a study of the KK 258 galaxy, an isolated transition type dwarf system situated at a distance of 2.23 ± 0.05 Mpc from the Milky Way. The distance to KK 258 was measured by applying the tip of the red giant branch method to V and I band images obtained with the Advanced Camera for Surveys on the Hubble Space Telescope. We discuss the star formation history of KK 258 derived from its colour-magnitude diagram. The main starburst in KK 258 apparently occurred 12 – 14 Gyr ago. The average rate of star formation in that period was $7.9_{-3.2}^{+4.8} \times 10^{-3} M_{\odot}/\text{yr}$. The average metallicity of the stars formed is quite low, $[\text{Fe}/\text{H}] \simeq -1.6$. About 70 per cent of the total stellar mass of the galaxy was formed during the initial starburst. A weak but reliable sign of star formation is seen also in the last billion years with an average rate of $3.8_{-1.0}^{+3.0} \times 10^{-4} M_{\odot}/\text{yr}$.

Previous observations of KK 258 in the $\text{H}\alpha$ line with the 6-meter Russian telescope revealed a faint emissive patch of ~ 5 arcsec size in the central region of KK 258. The integral flux from the patch corresponds to the star formation rate $\log[SFR] = -4.68$ in units of $[M_{\odot}/\text{yr}]$. This emission knot is also seen in ultraviolet images obtained with the space GALEX telescope yielding the star formation rate of $\log[SFR] = -4.48 M_{\odot}/\text{yr}$ in good agreement with the estimate from $\text{H}\alpha$ emission.

Additionally, spectroscopic observations with the SALT telescope identify KK 258 as possessing a heliocentric radial velocity $V_h = 92 \pm 5 \text{ km s}^{-1}$ or the Local Group centroid velocity $V_{LG} = 150 \text{ km s}^{-1}$. Under these velocity and distance, KK 258 has a low peculiar velocity ($V_{pec} \sim 3 \text{ km s}^{-1}$) with respect to the local Hubble flow with $H_0 = 73$

$\text{km s}^{-1} \text{ Mpc}^{-1}$, perturbed by the Local Group with the radius of zero velocity surface $R_0 = 0.9$ Mpc.

We compared KK 258 with 29 other nearby dwarf galaxies classified in the Updated Nearby Galaxy Catalog as been transition type. According to its basic parameters: the absolute magnitude of $M_B = -10.3$ mag, the average surface brightness of 26.0 mag arcsec^{-2} , the hydrogen mass of $\log(M_{\text{HI}}) < 5.75 M_{\odot}$, and the specific star formation rate of $\log[\text{sSFR}] = -2.74$ KK 258 looks like a typical representative of the sample of transition type dwarfs. However, unlike other dTr- galaxies, KK 258 is sufficiently isolated that tidal interactions are not likely to have affected its evolution in any way. From its spatial location KK 258 can be described as an outlier of the dwarf galaxy group around NGC 55, which contains 5 members and resides in the scattered Sculptor filament. The spatially nearest galaxy to KK 258 is a dwarf irregular galaxy UGCA 438 separated by 0.46 Mpc. The status of the dwarf system KK 258 in the category of isolated transition dwarfs seems difficult to explain by usual gas stripping mechanisms.

ACKNOWLEDGEMENTS

This work is supported by RFBR grants 13-02-90407 and 13-02-92960. LNM acknowledge the support from RFBR grant 13-02-00780 and Research Program OFN-17 of the Division of Physics, Russian Academy of Sciences. Observations of KK 258 were made with Hubble Space Telescope in the course of program GO-12546. Some of the observations reported in this paper were obtained with the Southern African Large Telescope (SALT), DDT program 2013-1-RSA_OTH-026. AYK acknowledge the support from the National Research Foundation (NRF) of South Africa. We are grateful to Dmitry Makarov for help and discussion of the star formation history of KK258.

REFERENCES

- Abazajian K. N., Adelman-McCarthy J. K., Agüeros M. A., Allam S. S., Allende Prieto C., An D., Anderson K. S. J., Anderson S. F., Annis J., Bahcall N. A., et al. 2009, ApJS, 182, 543
- Barmina R., Girardi L., Chiosi C., 2002, A&A, 385, 847
- Benítez-Llambay A., Navarro J. F., Abadi M. G., Gottlöber S., Yepes G., Hoffman Y., Steinmetz M., 2013, ApJ, 763, L41
- Buckley D. A. H., Swart G. P., Meiring J. G., 2006, in Society of Photo-Optical Instrumentation Engineers (SPIE) Conference Series Vol. 6267 of Society of Photo-Optical Instrumentation Engineers (SPIE) Conference Series, Completion and commissioning of the Southern African Large Telescope
- Burgh E. B., Nordsieck K. H., Koblunicky H. A., Williams T. B., O'Donoghue D., Smith M. P., Percival J. W., 2003, in Iye M., Moorwood A. F. M., eds, Instrument Design and Performance for Optical/Infrared Ground-based Telescopes Vol. 4841 of Society of Photo-Optical Instrumentation Engineers (SPIE) Conference Series, Prime Focus Imaging Spectrograph for the Southern African Large Telescope: optical design. pp 1463–1471

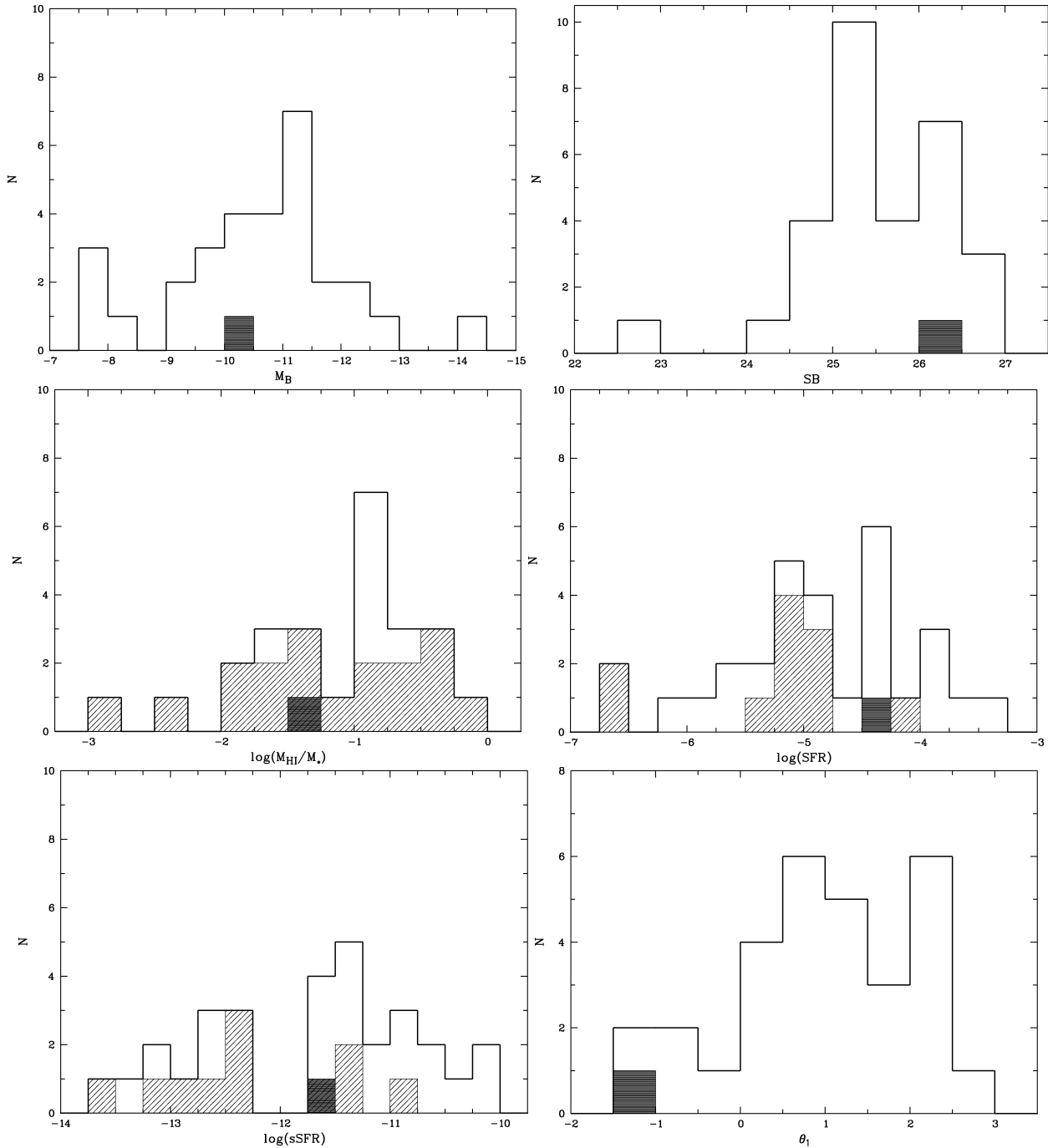


Figure 6. A mosaic of histograms showing the distribution of 30 dTr galaxies according to different parameters. KK 258 is marked in black. Upper limits of $M(\text{HI})$ and SFR are shaded

Chiboucas K., Jacobs B. A., Tully R. B., Karachentsev I. D., 2013, *AJ*, 146, 126

Chiboucas K., Karachentsev I. D., Tully R. B., 2009, *AJ*, 137, 3009

Crawford S. M., Still M., Schellart P., Balona L., Buckley D. A. H., Dugmore G., Gulbis A. A. S., Kniazev A., Kotze M., Loring N., Nordsieck K. H., Pickering T. E., Potter S., Romero Colmenero E., Vaisanen P., Williams T., Zitsman E., 2010, in *Society of Photo-Optical Instrumentation Engineers (SPIE) Conference Series Vol. 7737 of Society of Photo-Optical Instrumentation Engineers (SPIE)*

Conference Series, PySALT: the SALT science pipeline
 Gil de Paz A., Boissier S., Madore B. F., Seibert M., Joe Y. H., Boselli A., Wyder T. K., Thilker D., Bianchi L., Rey S.-C., Rich R. M., Barlow T. A., Conrow T., Forster K., Friedman P. G., et al. 2007, *ApJS*, 173, 185

Giovanelli R., Haynes M. P., Adams E. A. K., Cannon J. M., Rhode K. L., Salzer J. J., Skillman E. D., Bernstein-Cooper E. Z., McQuinn K. B. W., 2013, *AJ*, 146, 15

Girardi L., Bressan A., Bertelli G., Chiosi C., 2000, *A&AS*, 141, 371

Hidalgo S. L., Monelli M., Aparicio A., Gallart C., Skillman

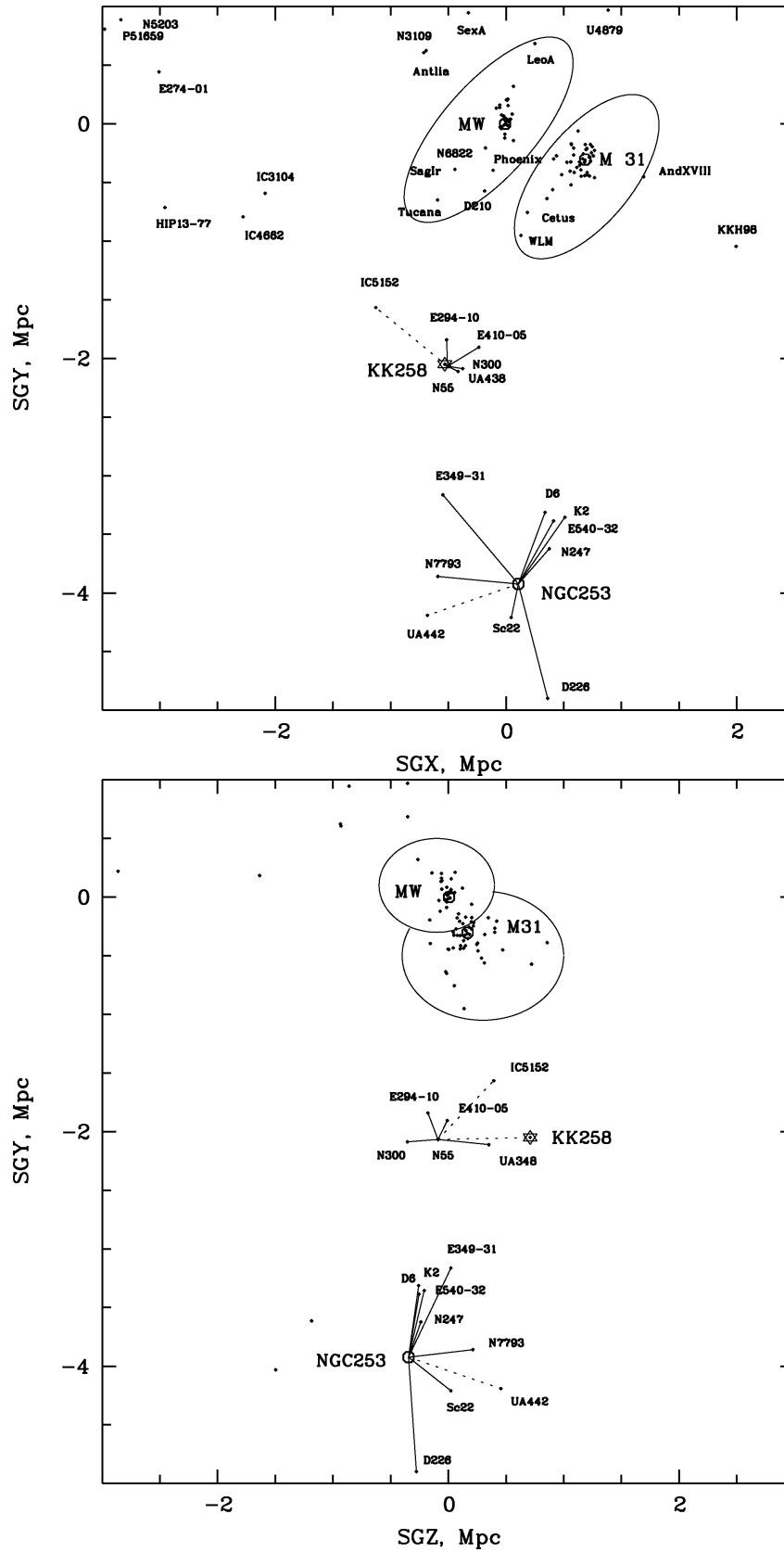


Figure 7. The distribution of known galaxies within a distance of 3 Mpc around the NGC 55 group in Supergalactic coordinates.

- E. D., Cassisi S., Bernard E. J., Mayer L., Stetson P., Cole A., Dolphin A., 2013, *ApJ*, 778, 103
- Ibata R., Martin N. F., Irwin M., Chapman S., Ferguson A. M. N., Lewis G. F., McConnachie A. W., 2007, *ApJ*, 671, 1591
- Ibata R. A., Lewis G. F., McConnachie A. W., Martin N. F., Irwin M. J., Ferguson A. M. N., Babul A., Bernard E. J., Chapman S. C., Collins M., Fardal M., Mackey A. D., Navarro J., Peñarrubia J., Rich R. M., Tanvir N., Widrow L., 2014, *ApJ*, 780, 128
- Jacobs B. A., Rizzi L., Tully R. B., Shaya E. J., Makarov D. I., Makarova L., 2009, *AJ*, 138, 332
- Jacobs B. A., Tully R. B., Rizzi L., Karachentsev I. D., Chiboucas K., Held E. V., 2011, *AJ*, 141, 106
- Kaisin S. S., Karachentsev I. D., 2013, *Astrophysical Bulletin*, 68, 381
- Karachentsev I., Kaisina E., Kaisin S., Makarova L., 2011, *MNRAS*, 415, L31
- Karachentsev I. D., Karachentseva V. E., Huchtmeier W. K., Makarov D. I., 2004, *AJ*, 127, 2031
- Karachentsev I. D., Kashibadze O. G., Makarov D. I., Tully R. B., 2009, *MNRAS*, 393, 1265
- Karachentsev I. D., Makarov D. I., Kaisina E. I., 2013, *AJ*, 145, 101
- Kennicutt Jr. R. C., 1998, *ARA&A*, 36, 189
- Kirby E. N., Cohen J. G., Bellazzini M., 2012, *ApJ*, 751, 46
- Klypin A., Kravtsov A. V., Valenzuela O., Prada F., 1999, *ApJ*, 522, 82
- Kniazev A. Y., Zijlstra A. A., Grebel E. K., Pilyugin L. S., Pustilnik S., Väisänen P., Buckley D., Hashimoto Y., Loaring N., Romero E., Still M., Burgh E. B., Nordsieck K., 2008, *MNRAS*, 388, 1667
- Kobulnicky H. A., Nordsieck K. H., Burgh E. B., Smith M. P., Percival J. W., Williams T. B., O'Donoghue D., 2003, in Iye M., Moorwood A. F. M., eds, *Instrument Design and Performance for Optical/Infrared Ground-based Telescopes Vol. 4841 of Society of Photo-Optical Instrumentation Engineers (SPIE) Conference Series*, Prime focus imaging spectrograph for the Southern African large telescope: operational modes. pp 1634–1644
- Kopylov A. I., Tikhonov N. A., Fabrika S., Drozdovsky I., Valeev A. F., 2008, *MNRAS*, 387, L45
- Makarov D., Karachentsev I., 2011, *MNRAS*, 412, 2498
- Makarov D., Makarova L., Rizzi L., Tully R. B., Dolphin A. E., Sakai S., Shaya E. J., 2006, *AJ*, 132, 2729
- Makarov D. I., Makarova L. N., 2004, *Astrophysics*, 47, 229
- Makarova L., Koleva M., Makarov D., Prugniel P., 2010, *MNRAS*, 406, 1152
- Martin N. F., McConnachie A. W., Irwin M., Widrow L. M., Ferguson A. M. N., Ibata R. A., Dubinski J., Babul A., Chapman S., Fardal M., Lewis G. F., Navarro J., Rich R. M., 2009, *ApJ*, 705, 758
- McConnachie A. W., 2012, *AJ*, 144, 4
- McQuinn K. B. W., Skillman E. D., Berg D., Cannon J. M., Salzer J. J., Adams E. A. K., Dolphin A., Giovanelli R., Haynes M. P., Rhode K. L., 2013, *AJ*, 146, 145
- Monelli M., Gallart C., Hidalgo S. L., Aparicio A., Skillman E. D., Cole A. A., Weisz D. R., Mayer L., Bernard E. J., Cassisi S., Dolphin A. E., Drozdovsky I., Stetson P. B., 2010, *ApJ*, 722, 1864
- O'Donoghue D., Buckley D. A. H., Balona L. A., Bester D., Botha L., Brink J., Carter D. B., Charles P. A., Christians A., Ebrahim F., Emmerich R., Esterhuysen W., Evans G. P., Fourie C., et al. 2006, *MNRAS*, 372, 151
- Rhode K. L., Salzer J. J., Haurberg N. C., Van Sistine A., Young M. D., Haynes M. P., Giovanelli R., Cannon J. M., Skillman E. D., McQuinn K. B. W., Adams E. A. K., 2013, *AJ*, 145, 149
- Rizzi L., Tully R. B., Makarov D., Makarova L., Dolphin A. E., Sakai S., Shaya E. J., 2007, *ApJ*, 661, 815
- Salpeter E. E., 1955, *ApJ*, 121, 161
- Schlafly E. F., Finkbeiner D. P., 2011, *ApJ*, 737, 103
- Schlegel D. J., Finkbeiner D. P., Davis M., 1998, *ApJ*, 500, 525
- Tonry J. L., Stubbs C. W., Lykke K. R., Doherty P., Shivers I. S., Burgett W. S., Chambers K. C., Hodapp K. W., Kaiser N., Kudritzki R.-P., Magnier E. A., Morgan J. S., Price P. A., Wainscoat R. J., 2012, *ApJ*, 750, 99
- Tully R. B., Rizzi L., Dolphin A. E., Karachentsev I. D., Karachentseva V. E., Makarov D. I., Makarova L., Sakai S., Shaya E. J., 2006, *AJ*, 132, 729
- Tully R. B., Rizzi L., Shaya E. J., Courtois H. M., Makarov D. I., Jacobs B. A., 2009, *AJ*, 138, 323
- Weisz D. R., Dolphin A. E., Dalcanton J. J., Skillman E. D., Holtzman J., Williams B. F., Gilbert K. M., Seth A. C., Cole A., Gogarten S. M., Rosema K., Karachentsev I. D., McQuinn K. B. W., Zaritsky D., 2011, *ApJ*, 743, 8
- Yang S.-C., Wagner-Kaiser R., Sarajedini A., Kim S. C., Kyeong J., 2014, *ApJ*, 784, 76

This paper has been typeset from a $\text{\TeX}/\text{\LaTeX}$ file prepared by the author.